Conference Paper, Published Version

Faghihirad, S.; Lin, B.; Falconer, Roger

3D layer-integrated modelling of flow and sediment transport through a river regulated reservoir

Verfügbar unter/Available at: https://hdl.handle.net/20.500.11970/99816

Vorgeschlagene Zitierweise/Suggested citation:
Faghihirad, S.; Lin, B.; Falconer, Roger (2010): 3D layer-integrated modelling of flow and sediment transport through a river regulated reservoir. In: Dittrich, Andreas; Koll, Katinka; Aberle, Jochen; Geisenhainer, Peter (Hg.): River Flow 2010. Karlsruhe: Bundesanstalt für Wasserbau. S. 1573-1580.

3D layer-integrated modelling of flow and sediment transport through a river regulated reservoir

S. Faghihirad, B. Lin & R. A. Falconer
School of Engineering, Cardiff University, Cardiff, U.K

ABSTRACT: Details are given of the refinement of a three-dimensional layer integrated $k - \varepsilon$ turbulence model and its application to a scaled physical model of a river regulated reservoir, named Hamidieh Reservoir. The strong turbulent flows generated in the regulated reservoir are due to the high volumes of flow diversion with low head differences. In this paper, the numerical model is applied to a regulated dam, associated with water intakes and sluice gates, with the aim being to investigate the flow patterns and sediment transport processes in the vicinity of these hydraulic structures. The calibration of the model is undertaken using measurements made from a scaled physical model. The numerical model is able to test various scenarios which are difficult to test in the physical model. In this context different scenarios are introduced to investigate the effects of different intake and sluice gate configurations, as well as their operation schemes on the flow and sediment transport processes in Hamidieh Reservoir. The results have shown that a non-uniform velocity distribution zone exists upstream of one of the intakes. Also, the sluice gates do not appear to have any considerable effect on the suspended sediments concentrations moving through the intakes.

Keywords: Numerical models; $k - \varepsilon$ model; Regulated reservoir; 3D flow; Laboratory tests.

1 INTRODUCTION

In reservoirs and rivers, in order to understand the impact of hydraulic structures on the hydrodynamic and sediment transport processes it is often necessary to investigate these processes in three dimensions. Currently, physical models are still widely used as an essential tool to obtain information about these processes. Generally speaking, physical models need a long time to construct and are expensive to run, particularly if large scales are involved. In the project presented in this paper a detailed numerical modelling investigation has been undertaken to simulate water flows through hydraulic structures and their interaction with sediments. Using a numerical model it is possible to examine various scenarios that are difficult to test in physical models. These scenarios are useful for hydraulic structure design and operation schemes and future maintenance.

River regulated reservoirs are often constructed downstream of dams, with relatively low elevations, to enable water to be distributed for water supply purposes. However, there are major differences between the low head regulatory reservoirs and those reservoirs that are associated with normal high dams, in that strong turbulence flows generated in the regulated reservoir are primarily due to high flow discharges. The turbulence may introduce complex flow patterns, which can be difficult to predict.

In recent years, a number of studies have been undertaken using two- and three- dimensional hydrodynamic models to achieve improved understanding of the role of hydraulic structures. Different types of numerical models, such as MIKE21, MIKE_3 and Delft3D, have been used to predict the impact of hydraulic structures on the hydrodynamic, sediment transport and morphological processes.

For the model simulations reported herein, predictions were obtained using a layer integrated three-dimensional hydrodynamic and sediment transport model. In this model a two-equation turbulence model was used, with details of the governing equations and boundary conditions being given. The original mathematical model was developed by Hakimzadeh and Falconer (2007)

for simulating re-circulating flows in tidal basins. Some improvements were made in the model in order to predicting the flow, sediment transport and morphological processes in a river flow regulated reservoir. These improvements enhance the capabilities of the exist model. The refined model was applied to the scaled physical model of Hamidieh regulated reservoir to obtain better understanding of the flow and sediment transport regime within the reservoir.

2 NUMERICAL MODEL

In this study, the numerical model used to predict the flow and sediment transport through a river regulated reservoir comprises two modules: a hydrodynamic module and a sediment transport module. The hydrodynamic governing equations are solved using a combined layer-integrated and depth-integrated scheme (Lin & Falconer, 1997), with the two-equation k-ε model being used for turbulence closure (Hakimzadeh & Falconer, 2007)). In the sediment transport module, the suspended sediment transport equation is solved using an operator splitting algorithm (Lin & Falconer, 1996).

2.1 Layer integrated hydrodynamic model

The governing equations used to describe flows in reservoirs are generally based on 3-D Reynolds equations for incompressible and unsteady turbulent flows. If the vertical acceleration of the flow is negligible in comparison with the gravity and the vertical pressure gradient terms, then the hydrostatic pressure distribution assumption can be made. As a first attempt, the density of the water has also been assumed constant throughout the computational domain. In applying these approximations, the three-dimensional governing equations of mass and momentum can be written respectively in their conservative form as follows:

$$\frac{\partial u}{\partial x} + \frac{\partial v}{\partial y} + \frac{\partial w}{\partial z} = 0 \tag{1}$$

$$\frac{\partial u}{\partial t} + \frac{\partial uu}{\partial x} + \frac{\partial uv}{\partial y} + \frac{\partial uw}{\partial z} = fv - \frac{1}{\rho}\frac{\partial p}{\partial x} + \frac{\partial(-\overline{u'u'})}{\partial x}$$

$$+ \frac{\partial(-\overline{u'v'})}{\partial y} + \frac{\partial(-\overline{u'w'})}{\partial z} \tag{2}$$

$$\frac{\partial u}{\partial t} + \frac{\partial vu}{\partial x} + \frac{\partial vv}{\partial y} + \frac{\partial vw}{\partial z} = -fu - \frac{1}{\rho}\frac{\partial p}{\partial y} + \frac{\partial(-\overline{v'u'})}{\partial x}$$

$$+ \frac{\partial(-\overline{v'v'})}{\partial y} + \frac{\partial(-\overline{v'w'})}{\partial z} \tag{3}$$

$$\frac{\partial p}{\partial z} + \rho g = 0 \tag{4}$$

where $t = $ time, $x, y, z = $ Cartesian co-ordinates, $u, v, w = $ components of velocity in the x, y, z direction, respectively, $p = $ pressure, $\rho = $ density of water, $f = $ Coriolis parameter, $g = $ gravitational acceleration and $-\overline{u'u'}, -\overline{u'v'}, -\overline{u'w'}, -\overline{v'u'}, -\overline{v'v'}, -\overline{v'w'} = $ Reynolds stresses in the $x-z$, $y-z$ plain, respectively.

A sketch of the 3D grid and relative positions of the governing variables in the $x-z$ plane are illustrated in Figure 1. As can bee seen from Figure 1 that there are three layer types including: the top, middle, and bottom layers. The free surface and bed topography are prescribed within the top and bottom layers, respectively, with both varying in thickness with the x, y coordinates so that they only include water ($m = $ the number of layers).
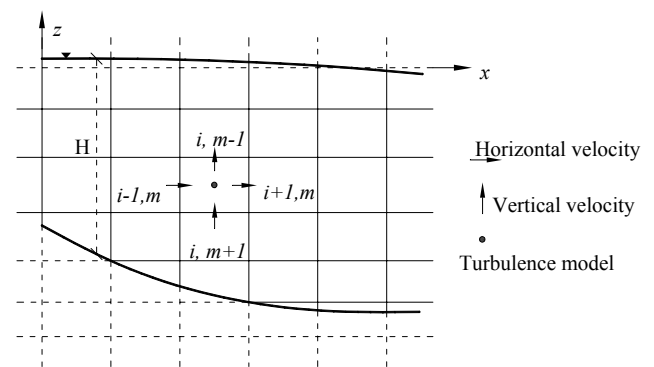

Figure 1. Coordinate system for layer integrated equations

2.2 Turbulence model

In the numerical model reported herein the eddy viscosity concept has been used to represent the Reynolds stresses. The horizontal eddy viscosity was equated to the depth averaged eddy viscosity, based on the horizontal velocity distribution derived from integrating the model predicted vertical velocity distributions.

For the two-equation turbulence model, the horizontal eddy viscosity was determined using the depth integrated $k-\varepsilon$ turbulence model, given as (Falconer and Li, 1994):

$$\frac{\partial \bar{k}H}{\partial t} + \frac{\partial \bar{k}UH}{\partial x} + \frac{\partial \bar{k}VH}{\partial y} = \frac{\partial}{\partial x}\left(\frac{\bar{v}_{th}H}{\sigma_k} \cdot \frac{\partial \bar{k}}{\partial x}\right) + \frac{\partial}{\partial y}\left(\frac{\bar{v}_{th}H}{\sigma_k} \cdot \frac{\partial \bar{k}}{\partial y}\right)$$

$$+ \bar{v}_{th}H\left[2\left(\frac{\partial U}{\partial x}\right)^2 + 2\left(\frac{\partial v}{\partial x}\right)^2\right]$$

1574

$$+\left(\frac{\partial U}{\partial y}+\frac{\partial V}{\partial x}\right)^2\right]+c_k U_*^3-\bar{\varepsilon}H \tag{5}$$

$$\frac{\partial\bar{\varepsilon}H}{\partial t}+\frac{\partial\bar{\varepsilon}UH}{\partial x}+\frac{\partial\bar{\varepsilon}VH}{\partial y}=\frac{\partial}{\partial x}\left(\frac{\bar{v}_{th}H}{\sigma_\varepsilon}\cdot\frac{\partial\bar{\varepsilon}}{\partial x}\right)+\frac{\partial}{\partial y}\left(\frac{\bar{v}_{th}H}{\sigma_\varepsilon}\cdot\frac{\partial\bar{\varepsilon}}{\partial y}\right)$$

$$+c_{1\varepsilon}c_\mu\bar{k}H\left[2\left(\frac{\partial U}{\partial x}\right)^2+2\left(\frac{\partial V}{\partial y}\right)^2\right.$$

$$+\left(\frac{\partial U}{\partial y}+\frac{\partial V}{\partial x}\right)^2\right]+c_\varepsilon\frac{U_*^4}{H}-c_{2\varepsilon}\frac{\bar{\varepsilon}^2}{\bar{k}}H \tag{6}$$

where $\bar{k}=$ depth average turbulent kinetic energy; $U, V =$ depth average velocity components in the x, y direction, respectively; and $\bar{\varepsilon}=$ depth average dissipation rate of kinetic energy. The key coefficients are given as:

$$c_k=(f/2)^{-1/2}, \quad c_\varepsilon=3.6c_{2\varepsilon}c_\mu^{1/2}(f/2)^{-3/4}, \quad \bar{v}_{th}=c_\mu\frac{\bar{k}^2}{\bar{\varepsilon}}$$

where $\sigma_k, \sigma_\varepsilon, c_\mu, c_{1\varepsilon}, c_{2\varepsilon}=$ constant coefficient; with $f=$ Darcy friction factor.

By assuming that $\hat{var}=(1/\Delta z)\int_{m+1/2}^{m-1/2}(var)dz$, where $m\pm1/2$ refer to the vertical elevations of the layer interface between the $m+1$, m and $m-1$ layers respectively such as $\hat{k}=(1/\Delta z)\int_{m+1/2}^{m-1/2}kdz$, then the vertical eddy viscosity can be evaluated using the layer integrated form of the $k-\varepsilon$ equations, as derived in Hakimzadeh (1997), giving

$$\frac{\partial\hat{k}\Delta z}{\partial t}\bigg|_m+\left(\frac{\partial\hat{k}q_{1x}}{\partial x}+\frac{\partial\hat{k}q_{1y}}{\partial y}\right)_m+\left(w\hat{k}\right)_{m-1/2}-\left(w\hat{k}\right)_{m+1/2}$$

$$=\left(\frac{\hat{v}_{tv}}{\sigma_k}\cdot\frac{\partial\hat{k}}{\partial z}\right)_{m-1/2}-\left(\frac{\hat{v}_{tv}}{\sigma_k}\cdot\frac{\partial\hat{k}}{\partial z}\right)_{m+1/2}+\hat{p}\Delta z-\hat{\varepsilon}\Delta z \tag{7}$$

$$\frac{\partial\hat{\varepsilon}\Delta z}{\delta t}\bigg|_m+\left(\frac{\partial\hat{\varepsilon}q_{1x}}{\partial x}+\frac{\partial\hat{\varepsilon}q_{1y}}{\partial y}\right)_m+\left(w\hat{\varepsilon}\right)_{m-1/2}-\left(w\hat{\varepsilon}\right)_{m+1/2}$$

$$=\left(\frac{\hat{v}_{tv}}{\sigma_\varepsilon}\cdot\frac{\partial\hat{\varepsilon}}{\partial z}\right)_{m-1/2}-\left(\frac{\hat{v}_{tv}}{\sigma_\varepsilon}\cdot\frac{\partial\hat{\varepsilon}}{\partial z}\right)_{m+1/2}+c_{1\varepsilon}\frac{\hat{\varepsilon}}{\hat{k}}\hat{p}\Delta z-c_{2\varepsilon}\frac{\hat{\varepsilon}^2}{\hat{k}}\Delta z \tag{8}$$

where

$$\hat{p}=\hat{v}_{tv}\left[\left(\frac{\partial\bar{u}}{\partial z}\right)^2+\left(\frac{\partial\bar{v}}{\partial z}\right)^2\right] \tag{9}$$

$$\hat{v}_{tv}=c_\mu\frac{\hat{k}^2}{\hat{\varepsilon}} \tag{10}$$

For the turbulence model equations the following boundary conditions were used:
(i) inlet: distribution of k and ε were given.
Demunren & Rodi (1983) suggested two formulae for fully developed channel flows:

$$k_d=0.004u_d^2 \tag{11}$$

$$\varepsilon_d=c_\mu^{3/4}\frac{k_d^{3/2}}{0.09b} \tag{12}$$

where $u_d=$ inflow velocity, and $b=$ inlet width
(ii) outlet: $\frac{\partial k}{\partial n}=0$ and $\frac{\partial\varepsilon}{\partial n}=0$

(iii) free surface: k and ε must be given
Krishnappan & Lau (1986) suggested for ε the following condition should be used:

$$\varepsilon_f=\frac{c_{f\varepsilon}\left(\frac{k_f}{\sqrt{c_\mu}}\right)^{3/2}}{\kappa z_f} \tag{13}$$

where $z_f=$ distance from the free surface to the grid centre, and $k_f=$ the corresponding value for the turbulent energy. The value of $c_{f\varepsilon}$ used in equation (13) is 0.164, $c_\mu=0.09$ and $\kappa=0.41$ is the von Karman constant.

2.3 Sediment transport equation

Depending upon the size and density of the bed material and the flow conditions, sediment particles can be transported by the flow in the form of bed load and suspended load. The 3-D mass equation for sediment in suspension is written as:

$$\frac{\partial S}{\partial t}+\frac{\partial}{\partial x}(uS)+\frac{\partial}{\partial y}(vS)+\frac{\partial}{\partial z}[(w-W_s)S]-\frac{\partial}{\partial x}\left(\varepsilon_x\frac{\partial S}{\partial x}\right)$$

$$-\frac{\partial}{\partial y}\left(\varepsilon_y\frac{\partial S}{\partial y}\right)-\frac{\partial}{\partial z}\left(\varepsilon_z\frac{\partial S}{\partial z}\right) \tag{14}$$

where $S=$ sediment concentration, $W_s=$ particle settling velocity, $\varepsilon_x, \varepsilon_y$ and $\varepsilon_z=$ sediment mixing coefficient in x, y, z direction, respectively. For suspended sand particles in the range of 100-1000 μm, the following equation was used to determine W_s (van Rijn, 1984):

$$W_s = 10 \frac{v}{D_s} \left\{ \left[1 + \frac{0.01(s-1)gD_s^3}{v^2} \right]^{0.5} - 1 \right\} \quad (15)$$

where v = kinematic viscosity for clear water, s = specific density of suspended sediment, and D_s = representative particle diameter of the suspended sediment particles.

The mixing coefficients were related to the turbulent eddy viscosity through the equations:

$$\varepsilon_x = \frac{v_{th}}{\sigma_h} , \; \varepsilon_y = \frac{v_{th}}{\sigma_h} \text{ and } \varepsilon_z = \frac{v_{tv}}{\sigma_v} \quad (16)$$

where σ_h, σ_v = Schmidt numbers is the horizontal and vertical directions respectively, with values ranging from 0.5 to 1.0.

In solving Eq. (14), four type of boundaries (inflow, outflow, water surface and sediment bed boundary) need to specified. For more study, those refer to Lin and Falconer (1997). The important assumption for a moveable bed contains that in zones where the fluid flow is varying rapidly or in (circulation) zones where the velocities are too small to initiate sediment motion, the application of an instantaneously adjusted equilibrium bed concentration may result in a positive concentration gradient near the bed. In the current model the main focus is the sediment transport. A fixed bed was assumed, but mass of bed sediment changes due to erosion and deposition was recovered.

3 PROJECT BACKGROUND

Hamidieh regulated reservoir is located 11 km away from Hamidieh Town. It is located on the Karkhe River, downstream of Karkhe reservoir dam. There are two water intakes, named Ghods and Vosaileh intakes. Currently, the Vosaileh water intake channel is 10.8 km long with a maximum discharge of 60 m^3/s while Ghods operates with a 2.5 km long channel with a maximum discharge capacity of 13 m^3/s.

Due to the development in irrigation and drainage network of Azadegan and Chamran regions, the present conditions of the water intakes are not able to meet the water demand. Hence, it is necessary to increase the flow rate from these intakes by building new water intake structures.

Hamidieh reservoir dam is 192 m long, 4.5 m high with 19 spillway bays and 10 sluice gates. Azadegan is to replace Ghods water intake with an inlet width of 56 m, 8 opening bays and 4 under sluice gates. It is intended to increase the discharge capacity from 13 m^3/s to 75 m^3/s. Vosaileh water intake is also to be replaced by Chamran with an inlet width of 86.6 m, 16 opening bays and 13 trash racks opening to increase the dis-

charge capacity from 60 m^3/s to 90 m^3/s. Figure 2 shows a plan view of Hamidieh regulated reservoir and associated structures. An undistorted 1/20-scale physical model of Hamidieh regulated reservoir and its relevant structures was constructed in 2002. The aim of project is to investigate the operation of the entire system and to improve the understanding of flow and sediment behaviors near the structures.
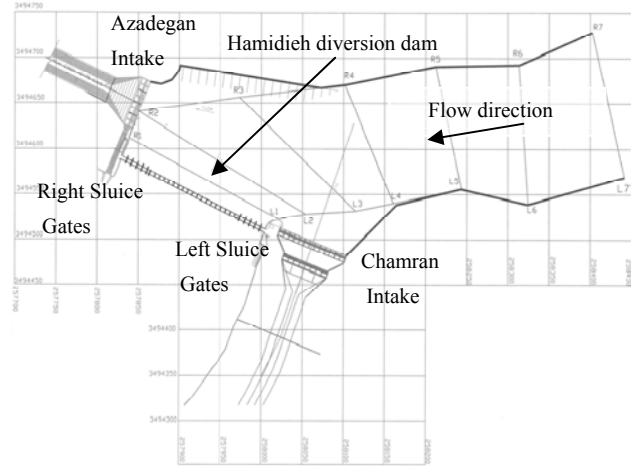

Figure 2. Plan of Hamidieh regulated dam

4 NUMERICAL SIMULATION

4.1 *Part one: hydrodynamics*

Details are first given below of the numerical modelling study of the hydrodynamic processes in the Hamidieh regulated reservoir. The model simulation was based on field surveyed data and measurement data obtained from the physical model for various operation conditions of the intakes and sluice gates. The results include the general flow patterns and more detailed velocity distributions within the reservoir and in the vicinity of hydraulic structures. The bathymetry data and hydrodynamic scenarios were defined by using field surveyed data and laboratory data. Figure 3 shows the bathymetry of the reservoir and the intakes based on the physical model scale.

One dredging zone in front of Azadegan intake close to the right bank has been recommended in order to make stable diversion flow into the intake for the long term water supply operation. Numerical and physical model simulations have been undertaken to investigate the feasibility of this measure in improving the condition for supplying water.

Table 1 lists the hydraulic parameters used to set-up the numerical model for testing hydrodynamic model scenarios. These parameters were chosen on the basis of the data obtained from the physical model experiments, in which the velocity

distribution was measured in front of the two intakes. The locations of these points are shown in the Figures 4 and 5.
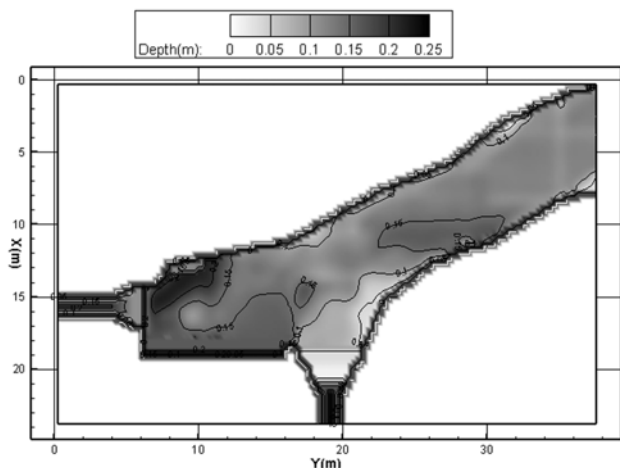

Figure 3. Bathymetry of Hamidieh, physical model scale

Table 1. The characteristic for the hydrodynamic scenario

	Hydraulic Boundary Condition	Turbulence Boundary Condition	Operation
Reservoir	Discharge 82.2 liter/s	Surface and Inlet	Water level (1.01 m)
Az. Intake	Discharge 41.9 liter/s	Outlet	
Ch Intake	Water Level (1 m)	Outlet	
L S	Closed	-	
R S	Closed	-	

Az Intake= Azadegan Intake, Ch Intake= Chamran Intake, L S= Left sluice gate and R S = Right sluice gate

The investigation of velocity distribution in the reservoir and the vicinity of the intakes presented a platform for studying the hydrodynamic behavior. In the physical model study the velocity was measured in front of the intakes at several points by current-meters. The location of these points is shown in the Figures 4 & 5. In this study, the velocity measurements at these points, together with the observed water surface levels were used for calibrating the hydrodynamic model.
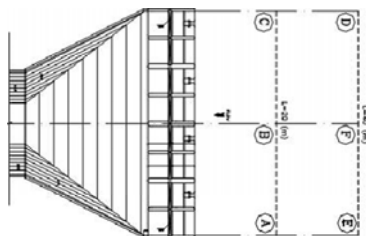

Figure 4. Location of velocity measuring points in vicinity of Azadegan intake

In the physical model study, the velocity was measured by a current-meter at $0.6D$ ($D=$ water depth) from the water surface and fitted to the physical scale. This depth had been chosen based on velocity logarithmic profile assumption for measuring mean velocity.
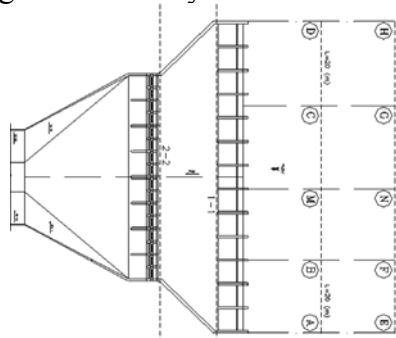

Figure 5 The location of velocity measuring points in the vicinity of Chamran intake

In applying the 3D layer integrated model to this case study the water depth was divided into 5 layers. The thickness of each layer was set to 0.057m, except for the top layer which was 0.051m in the main channel. The grid size was selected 0.25m. The water surface level was calibrated with the differences between the observed water surface levels obtained from the physical model and calculated by the numerical model being between 0.0022m and 0.0055m (Roughness parameter is used for calibrating water level regard to the physical tests). Table 2 indicates the velocity values for different locations that were pointed in Figures 4 and 5 for both the physical and the numerical models.

Table 2. Comparison between velocity values obtained from numerical and physical models

Location	Points	Measured (cm/s)	Calculated (cm/s)
Chamran	A	3.09	4.0
	B	5.91	6.08
	M	6.59	7.21
	C	5.91	6.63
	D	3.10	3.89
	E	3.08	3.86
	F	5.27	5.94
	N	6.40	7.24
	G	5.18	6.53
	H	3.59	3.89
Azadegan	A	3.97	4.70
	B	4.13	4.31
	C	4.46	5.15
	E	3.18	3.54
	F	4.25	3.73
	D	3.18	3.59

The physical model study and the numerical model simulation were not carried out simultaneously. In this research, efforts have been made to use the measured data for better calibration but it was not possible to test and measure hydraulic parameters for more scenarios and locations. Despite these limitations, the comparisons made using the available data in table 2 shows that the trend and quantities of velocity values obtained from the numeri-

cal and physical models are in an acceptable level of agreement for this complicated situation. In this hydrodynamic scenario 24 gates operated simultaneously and with a real bathymetry being used. The numerical results show that the magnitude of the vertical eddy viscosity is from 10 up to 500 times larger than the corresponding horizontal eddy viscosity in different areas.

The results obtained from both physical and numerical models are presented for the undistorted 1:20-scale model of Hamidieh regulated reservoir. The flow pattern and velocity contours in the reservoir were calculated by the numerical model and illustrated in Figure 6. The speed profiles along the depth predicted by the numerical model at 4 points near of the intakes (B&F for Azadegan and M&N for Chamran) were shown in figure 7. The measured velocity at $0.6D$ from the water surface in the physical model is also shown in this diagram.
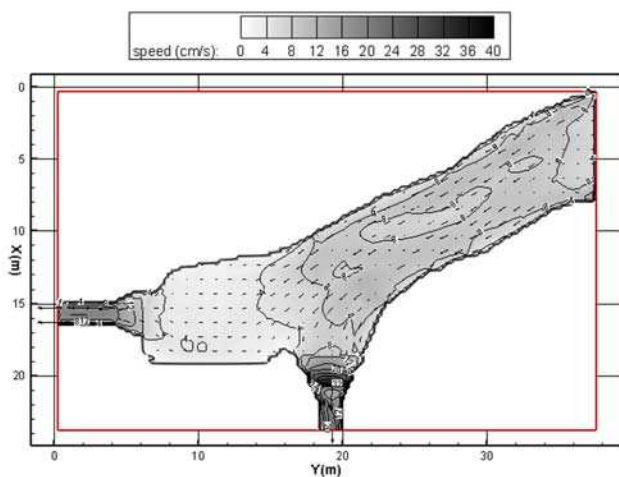

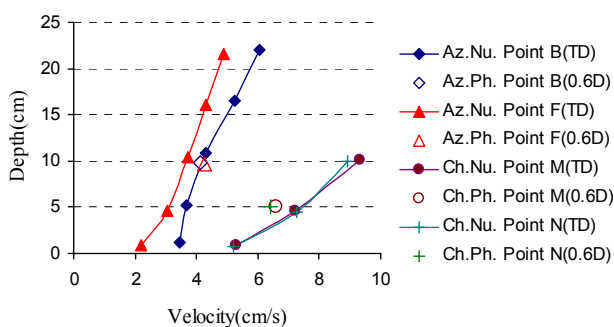Figure 6. Numerical model predicted flow pattern and speed contours

Figure 7. Model predicted velocity distributions and measured velocities at 0.6D from water surface (Az=Azadegan Intake, Ch=Chamran Intake, Nu=Numerical, Ph=Physical and TD=Total Depth)

From Figure 7 it can be seen that the mathematical model predicted velocity values agree reasonably well with measured ones from the physical model although some variations can be observed. An analysis of the hydrodynamic results identifies two main issues:

- According to the observation of the flow direction, it is noticed that a non-uniform velocity distribution zone exists upstream of Chamran intake on the left bank side. This is thought to be related to the location of the intake.
- The velocity pattern for the regulatory condition at the artificial dredging zone (in front of Azadegan intake) suggests that this is a location for high potential sedimentation.

4.2 Part two: sediment transport

For simulating sediment transport in hydraulic systems information such as particle size distribution, inflow discharge and associated sediment discharge, type of sediments (cohesive or non-cohesive) and understanding the dominant process of sediment transport (suspended load or bed load) in the nature are required. Previous studies have showed that the suspended transport is the dominant process for this case. The majority of sediment found in this region belongs to non-cohesive type. One of the most important tasks is to prevent sediments from entering the intakes. Any sediment particles deposited into the irrigation canals would cause a decrease in the flow rate. Currently, the stakeholders of the irrigation network have to dredge the canals periodically. In designing the new system of Hamidieh dam a great effort has been made to mitigate the sedimentation problem in canals.

In this research, different scenarios were considered in order to determine the amount of sediments entering the intakes. Details are given below of the numerical study of sediment transport process. The numerical model predictions were compared to the physical model results at three sites. The plan of these sites is shown in Figure 8.

In the numerical model, the scenarios were selected on the basis of the laboratory tests. van Rijn's (1984) formula was used to calculate the sediment transport rate. The patterns of the suspended sediments concentrations are shown in Figures 9, 10 for scenarios 2 and 3, respectively. The suspended sediment concentrations computed by the numerical model have demonstrated a good agreement with the ones measured from the physical mode (A maximum error is less than 21.3% and an averaged error is less than 7% that seems acceptable considering the overall complexity of the sediment transport). The sampling of suspended sediment concentration in the physical model was taken on the whole depth and calculated using a depth integrated formula. Table 4 shows a comparison between the measured and calculated suspended sediments concentrations in different points shown in Figure 8. The results ex-

press the movement of suspended sediment in the reservoir and over the intakes.
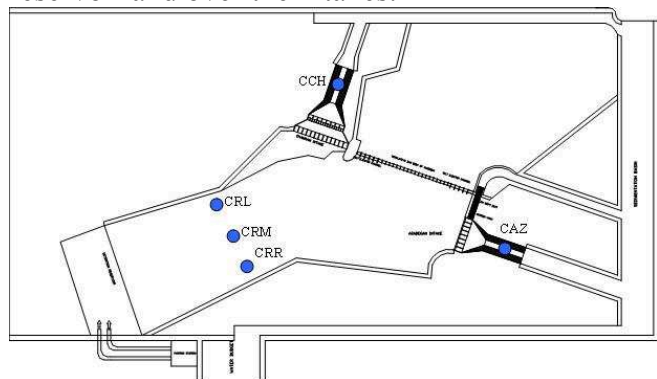

Figure 8. Location of measured sediment concentration points (CAZ=Concentration in Azadegan Intake, CCH=Concentration in Chamran Intake and CRR, CRM & CRL=Concentration in the reservoir)

Table 3 Main parameters for sediment scenarios

No		Operation	Boundary Condition	Concentration gr/liter
S.1	Reservoir	Water level 1.0225 m	Discharge 87.2 liter/s	0.4724
	Az Intake	-	Discharge 41.9liter/s	-
	Ch Intake	-	Water level 1 m	-
	L S	-	-	-
	R S	-	-	-
S.2	Reservoir	Water level 1.0225 m	Discharge 92.2 liter/s	0.6724
	Az Intake	-	Discharge 41.9 liter/s	-
	Ch Intake	-	Water level 1 m	-
	L S	-	Discharge 5.6 liter/s	-
	R S	-	-	-
S.3	Reservoir	Water level 1.0225 m	Discharge 135 liter/s	1.3391
	Az Intake	-	Discharge 41.9 liter/s	-
	Ch Intake	-	Water level 1 m	-
	L S	-	Discharge 25.2 liter/s	-
	R S	-	Discharge 25.2 liter/s	-
General data	d_{16}, d_{50}, d_{84} & $d_{90} = 0.0015, 0.0076, 0.0166$ & $0.0236 mm$ $Sepecific Gravity = 2.67$, $Grid\ size= 0.25\ m$ and $Computational\ time=360\ min\ with\ Intel(R)$ $Core(TM)2\ Quad\ CPU\ Q8400\ @\ 2.66\ GHz$			

Az Intake= Azadegan Intake, Ch Intake= Chamran Intake, L S= Left sluice gate and R S = Right sluice gate

Details are given of the model scenarios for simulating sediment transport in the case study. The scenarios are designed in three categories. The characteristics of these scenarios are:
- Low flow condition without sluice gates (S.1).
- Low flow condition with one sluice gate (S.2).

- High flow condition with sluice gates in both sides of the dam in operation (S.3).

The attributes of the scenarios are presented in table 3. The results showed that the suspended load has an important role in the sediment transport process and is closely related to particle size. A good agreement has been observed between the SSCs obtained from numerical and the physical models. The analysis of the sediment transport results identifies that:

(i) The suspended sediment concentration in Chamran intake is higher than the one in Azadegan intake. The main reason is thought to be the location of the intakes. Chamran intake is located in the internal curve position when considering the layout of the system.
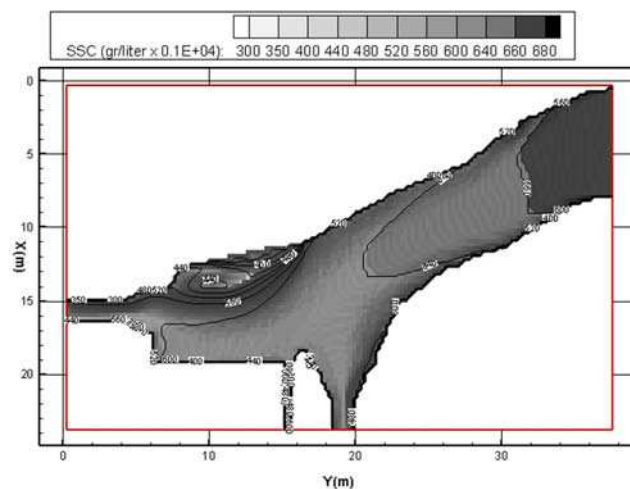

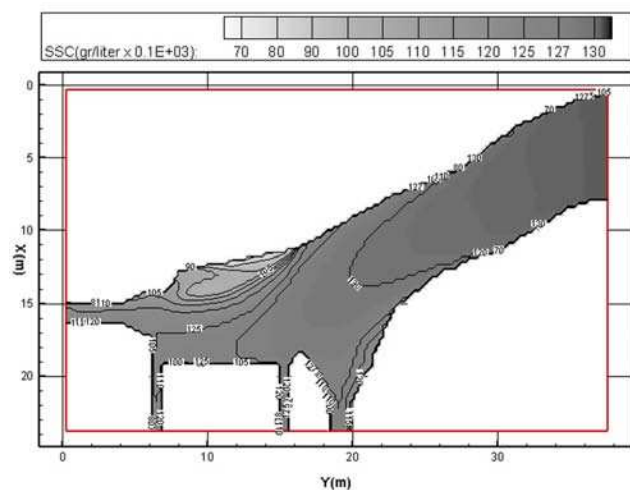Figure 9. Pattern of suspended sediments concentrations (SSC), scenario 2.

Figure 10. Pattern of suspended sediments concentrations (SSC), scenario 3.

(ii) The pattern of the suspended sediment movement in the reservoir has showed that the sediment entering rate to Chamran intake is affected very little by the sluice gate operation schemes. It means that the sluice gates on the left side do not have a considerable effect on reducing the suspended sediment concentration moving through Chamran intake.

(iii) It seems that the problem of sediment entering the intakes is remained. The layout of these hydraulic structures is only part of the reason for this problem. The natural system of sediment transport and the size of the sediments have an important role for this situation.

5 CONCLUSION

Details are given of the application of a three-dimensional numerical model to predict the flow and sediment transport through a river regulated reservoir. The aim of the study was to improve the understanding of the abilities of such numerical models in simulating these complex processes in a real case. An enhanced model was used to represent the complex flow pattern in the vicinity of hydraulic structures.

Table 4. SSC measured and predicted at sampling points

Scenarios	Points	SSC (Measured) gr/liter	SSC (Calculated) gr/liter
Scenario 1	CRL	0.401	0.452
	CRM	0.423	0.456
	CRR	0.417	0.452
	CAZ	0.396	0.401
	CCH	0.433	0.434
Scenario 2	CRL	0.563	0.645
	CRM	0.638	0.651
	CRR	0.605	0.645
	CAZ	0.618	0.589
	CCH	0.681	0.619
Scenario 3	CRL	1.18	1.3
	CRM	1.38	1.31
	CRR	1.12	1.3
	CAZ	0.99	1.20
	CCH	1.11	1.25

SSC= Sediment suspended sediment

A series of scenario runs of the operation schemes for Hamidieh regulated reservoir have revealed the governing phenomena in the system to a certain extent. The results obtained from the numerical model runs confirm that:
(i) A non-uniform velocity distribution zone exists upstream of Chamran intake on the left bank side.
(ii) The recommended artificial dredging zone, located in the front of Azadegan intake, will not affect the hydraulic behavior significantly.
(iii) The location of Chamran intake has a considerable impact on the suspended sediment concentration moving through the intake.
(iv) The sluice gates' operation scheme has very small impact on the suspended sediment flux entering into Chamran intake.
(v) The calibrated numerical model has been used to predict the water flow and sediment fluxes. Several scenarios were considered, with the numerical model results being used jointly with the experimental results to assist in the hydraulic design of the reservoir.

REFERENCES

Demuren, A.O., Rodi, W. 1983. Side discharges into open channels: Mathematical Model. Journal of Hydraulic Engineering, v 109, n 12, p 1707-1722.

Atkinson, E., Lawson, JD., Tosswell, P. 1994. Comparison of physical and computer modelling of the Kapunga intake with performance of the prototype. Hydraulic Research Walingford, UK, Reprot no. ODP121.

Falconer, R. A., Li, G. 1994. Numerical Modelling of tidal eddies in coastal basins with narrow entrance using turbulence model. Mixing and transport in the environment, K. J. Beven et al., eds., Wiley, London, 325-350

Hakimzadeh, H. 1997. Turbulence modelling of tidal currents in rectangular harbors. Ph.D. thesis, Univ. of Bradford, Bradford, U.K.

Hakimzadeh, H., Falconer, R. A. 2007. Layer integrated modelling of three-dimnesional recirculating flows in model tidal basins. Journal of water, port, coastal and ocean engineering; DOI: 10.1061/(ASCE)0733-950X.

Krishnappan, B. G., Lau, Y. L. 1986. Turbulence modelling of flood plain flows. Journal of hydraulic engineering, v 112, n 4, p 251-266.

Lin, B., Falconer, R. A. 1996. Numerical modelling of three dimensional suspended sediment for estuarine and coastal waters. Journal of hydraulic research. 34(4), 435-456.

Lin, B., Falconer, R. A. 1997. Three-dimensional layer integrated modelling of estuarine flows with flooding and drying. Estuarine, coastal and shelf science, 44, 737-751.

Water and Electricity Organization of Khuzestan Province (WEOKP). 2001. Karkhe irrigation network operation company, Bulletin No. 31, p 23-31.

Water Research Institute. 2002. Physical model of Hamidieh regulated reservoir. Report No. 223-76, 148p.

Van Rijn, L. C. 1984. Sediment transport, part II: suspended load transport. J. Hydraulic Eng. (ASCE), 110(11), 1613-1641.

Van Rijn, L. C. 1986. Mathematical modelling of suspended sediment in non-uniform flows. J. Hydraulic Eng. (ASCE), 112(6), 433-455